Journal of Engineering and Applied Sciences 14 (14): 4940-4950, 2019
ISSN: 1816-949X

Multi Response Optimization of Pulsed Gas Metal ARC Welding Process Parameter of AISI 904 L Super Austenitic Stainless Steel using Topsis Approach

P. Manavalan and S. Ravi
Department of Manufacturing Engineering, Annamalai University, 608002 Annamalai Nagar, India

Abstract: A study was carried out on Pulsed Gas Metal Arc Welding (P-GMAW) of AISI 904 L super austenitic stainless steel with a thickness of 5 mm and a filler wire of diameter of 1.2 mm. The joints were made with different process parameters, peak current (I_p), pulse time (t_p), pulse frequency (f), back ground current (I_b) and welding Speed (S) were considered as the input responses. Central composite rotatable design was used to carry out the experimental design and predict the effects of input and output responses. The processed joints were evaluated to obtain good welded joints in terms of good bead profile and mechanical properties such as bead width, tensile strength, percentage of elongation, impact strength and micro hardness of the welds which were considered as the output responses. Super Austenitic Stainless Steel (SASS) normally contains high amount of Mo, Cr, Ni, N and Mn. In order to solve a multi response optimization problem, the traditional Taguchi approach is not sufficient to get more appropriate results. To get appropriate and accurate results, a multi criteria decision making approach, namely, Techniques for Order Preference by Similarity to Ideal Solution (TOPSIS) technique was preferred and the same was applied in the present study. The Analysis of Variance (ANOVA) was carried out to investigate the significant process parameter for the pulsed gas metal arc welding process. Confirmation experiment was also conducted to validate the optimized parameters obtained from TOPSIS.

Key words: Pulsed gas metal arc welding, super austenitic stainless steel, TOPSIS, peak current, pulse frequency, ANOVA

INTRODUCTION

The use of conventional GMAW has traditionally been restricted by its inherent limitation in the control of metal transfer. The stable spray mode of metal transfer that offers the greatest ease of operation with high weld quality is possible only at higher welding current. Therefore, metal transfer in conventional GMAW cannot be regulated as independent of heat input but in Pulsed Gas Metal Arc Welding (P-GMAW) process, due to intermittent pulses of high current, spray transfer may be obtained at a comparatively lower level of heat input. In this process, current is periodically modulated between a lower level of base current and a higher level of peak current. Super austenitic stainless steel is the preferred material for high corrosion resistance requirements. This steel bridges the gap between relatively costlier austenitic stainless steel and expensive nickel base super alloys. The microstructure of Super Austenitic Stainless Steel (SASS) consists of a fully austenitic structure in the solution-quenched condition. The selection of the welding process parameters is very essential for obtaining the good weld. The main challenge for the manufacturer is in choosing the process input parameters that would produce an excellent weld joint. Conventionally, defining the weld input parameters (for newly welded products) to produce a welded joint with the required specifications is a time consuming process involving error development effort and the skill of the welding engineer or welding machine operator in choosing the right weld input parameters.

Laser beam welding of AISI 904 L super austenitic stainless steel with three different shielding gases (Argon, Helium and Nitrogen) was carried out with butt joints of full factorial design with three factors (beam power, travel speed and focal position). The model was developed to predict the Depth of Penetration (DP), Bead Width (BW) and Tensile Strength (TS) through artificial neural networks technique for three different environments (Argon, Helium and Nitrogen). This model was evaluated by means of percentage deviation between the predicted values and the actual values. The researchers concluded that there is a good agreement between the theoretically predicted (GA) and

Corresponding Author: P. Manavalan, Department of Manufacturing Engineering, Annamalai University, 608002 Annamalai Nagar, India

experimentally obtained values of tensile strength, depth of penetration and bead width (Sathiya *et al*., 2012). In laser welding of AISI 904 L super austenitic stainless steel parameters were optimized through grey relational grade analysis and desirability analysis methods. The investigators found that based on ANOVA results, both analyses were accurate techniques to optimize the laser welding process in order to obtain the good tensile strength. And also laser beam power is the most significant parameter followed by an interaction effect of beam power and travel speed, travel speed and focal position forhelium shielding gas. The interaction effect of beam power and travel speed has more influence than other factors followed by beam power, travel speed and focal position for argon and nitrogen shielding gases (Sathiya *et al*., 2011). In Tungsten Inert Gas welding (TIG) of Supermartensitic Stainless Steel (SMSS), parameters were optimized using Technique for Order Preference by Similarity to Ideal Solution method (TOPSIS). In conclusion, TOPSIS is suggested for optimisation of welding parameters in TIG welding of SMSS. Comparatively, 6th experimental run i.e., current = 160 A, Voltage = 18 V, travel speed = 55 mm/min, shielding gas flow rate = 14 lpm resulted in better quality of the weld (Chellappan *et al*., 2017).

The study was focused on welding of super austenitic stainless steel sheet using gas metal arc welding process with AISI 904 L super austenitic stainless steel with a solid wire of 1.2 mm diameter. The welding trial was performed with Box-Behnken design technique. The input parameters namely gas flow rate, voltage, travel speed and wire feed rate were selected and the corresponding output variables were Bead Width (BW), Bead Height (BH) and Depth of Penetration (DP). Based on the experimental data, mathematical models were developed as per regression analysis using Design Expert 7.1 Software. They developed a model based on minimizing the bead width and bead height and maximizing the depth of penetration using Genetic algorithm (Sathiya *et al*., 2013).

However, there are no visible published documents about the parameter optimization of P-GMAW using TOPSIS methodology. In the current research, an attempt has been made to develop a TOPSIS Model in order to predict the tensile strength, percentage of elongation, impact strength, bead width and micro hardness of the weld as a function of key output parameters in the P-GMAW process. A central compact factorial design was employed to identify the input parameters and to compare their influences on the tensile strength, percentage of elongation, impact strength, bead width and micro hardness of the weld to find which one is most significant. The results obtained from this model were then compared to experimental results.

MATERIALS AND METHODS

Experimental procedure: The welding trials were carried out on 5 mm thick sheet of AISI 904 L super austenitic stainless steel. The chemical composition of the base material is presented in Table 1. Super austenitic stainless steel filler wire of diameter of 1.2 mm was used. Butt weld experiments were conducted on 150×75×5 mm thick sheets. Joints prior to welding contact surfaces were cleaned with fresh stainless steel wire brush, followed by acetone swabbing.

Welding: The 5 mm thick AISI 904 L super austenitic stainless steel sheets were butt welded by pulse GMAW process with argon as shielding gas. The plates were rigidly fixed to avoid distortion during welding. Single V groove joint design was used. The welding parameters used for present investigations are given in Table 2. The other parameters were kept as constant (wire feed rate-6.5 m/min, shielding gas flow rate-15 lpm, stand of distance-1.5 mm/v groove angle-60°). The actual levels of the variables for each of the 30 experiments in the central composite rotatable design matrix are given in Table 3.

P-GMAW joints: The P-GMAW welds are shown in Fig. 1. Weld profiles were obtained by sectioning and polishing with suitable abrasive and diamond paste.

Weld samples were etched with 10% oxalic acid, an electrolyte to state and increase the contrast of the fusion zone with the base metal. The bead width and depth of penetrations were measured by optical microscopy and some of the bead profiles are shown in Fig. 2a-j.

From Fig. 2a-j it is perceived that in most of the bead profiles, the depth of penetration is obtained to full thickness of the sheet. Hence, from bead morphology i.e., bead width isalone taken to account for optimization. Full penetration of the jointsis essential for tensile strength. The tensile samples were prepared according to the AWS B 4.0 sub standards and tests were carried out at room temperature using Hounsfield Tensometer. In order to evaluate the Charpy impact toughness values of welded joints, a series of Charpy V-notch test was carried out on P-GMAW joints at room temperature. The specimens for Charpy test were taken perpendicular to weld direction according to the ASTM; E23. Notches were prepared exactly at the midpoint of the weld. Impact test was conducted for all welded samples and the value of the impact strength was recorded. The microhardness of weldment was measured in transverse direction using a Metco SMV 1000 Micro Vickers Hardness machine under 1-kg load, maintained for dual time 15 sec. The measured

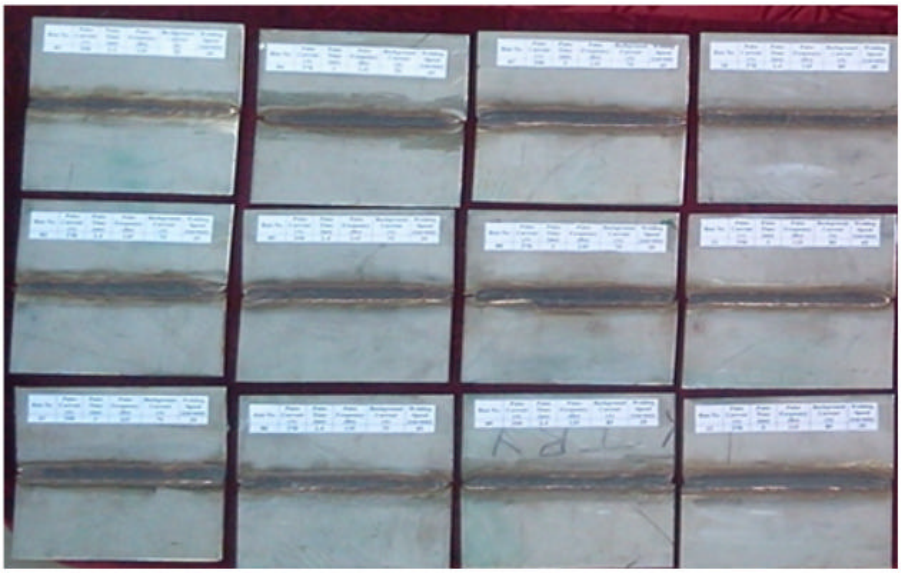

Fig. 1: Photograph views of P-GMAW joints

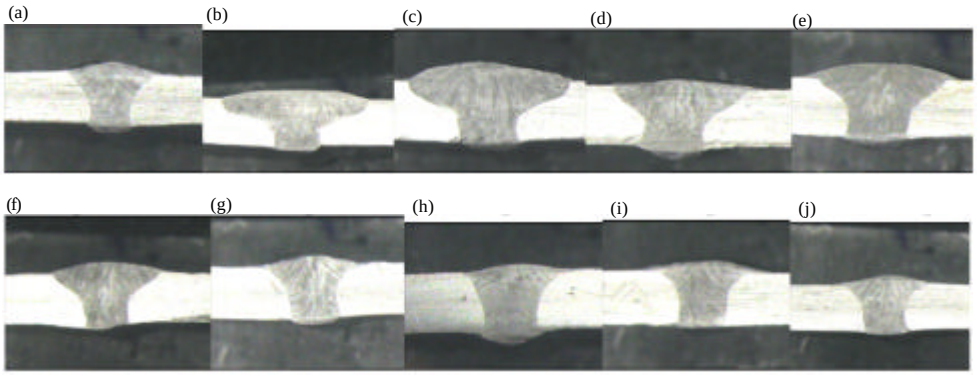

Fig. 2: Typical weld bead profiles of the joints: a) Exp. No 1; b) Exp. No 2; c) Exp. No. 6; d) Exp. No 9; e) Exp. No 14; f) Exp. No. 16; g) Exp. No 17; h) Exp. No 19; i) Exp. No 22 and j) Exp. No 27

Table 1: Base material chemical composition (weight in percentage)

Material	Si	Mn	P	S	Cr	Ni	Mo	C	Cu	Nb	V	Co	Fe
904L	0.409	1.402	0.035	0.021	20.850	23.125	4.102	0.020	1.327	0.023	0.066	0.017	47.886

Table 2: Welding process parameters and their levels

Parameters	Symbols	-2	-1	0	1	2
Peak current	I_p	340	350	360	370	380
Pulse time	t_p	2.1	2.4	2.7	3	3.3
Pulse frequency	f	120	125	130	135	140
Background current	I_b	70	75	80	85	90
Welding speed	S	30	35	40	45	50

experimental results i.e., tensile strength, percentage of elongation, hardness, impact strength and bead width of the welds are shown in Table 4.

TOPSIS methodology: Technique for Order Preference by Similarity to Ideal Solution method (TOPSIS) is one of the Multi Criteria Decision Making methods (MCDM) which is used to solve the type of decision making problem. This method is based on the concept that the chosen alternative should have the shortest Euclidean distance from the ideal solution and the farthest from the negative ideal solution. The ideal solution is a hypothetical solution for which all attribute values correspond to the maximum attribute values in the database comprising the satisfying solutions; the negative ideal solution is the hypothetical solution for which all attribute values correspond to the minimum attribute values in the

Table 3: Coded and actual levels of the five variables

Experiment No.	I_p	t_p	f	I_b	S	I_p(amps)	t_p(sec)	f(Hz)	I_b(amps)	S(mm/sec)
Factorial point										
01	-1	-1	-1	-1	1	350	2.4	125	75	45
02	1	-1	-1	-1	-1	370	2.4	125	75	35
03	-1	1	-1	-1	-1	350	3	125	75	35
04	1	1	-1	-1	1	370	3	125	75	45
05	-1	-1	1	-1	-1	350	2.4	135	75	35
06	1	-1	1	-1	1	370	2.4	135	75	45
07	-1	1	1	-1	1	350	3	135	75	45
08	1	1	1	-1	-1	370	3	135	75	35
09	-1	-1	-1	1	-1	350	2.4	125	85	35
10	1	-1	-1	1	1	370	2.4	125	85	45
11	-1	1	-1	1	1	350	3	125	85	45
12	1	1	-1	1	-1	370	3	125	85	35
13	-1	-1	1	1	1	350	2.4	135	85	45
14	1	-1	1	1	-1	370	2.4	135	85	35
15	-1	1	1	1	-1	350	3	135	85	35
16	1	1	1	1	1	370	3	135	85	45
Axial point										
17	-2	0	0	0	0	340	2.7	130	80	40
18	2	0	0	0	0	380	2.7	130	80	40
19	0	-2	0	0	0	360	2.1	130	80	40
20	0	2	0	0	0	360	3.3	130	80	40
21	0	0	-2	0	0	360	2.7	120	80	40
22	0	0	2	0	0	360	2.7	140	80	40
23	0	0	0	-2	0	360	2.7	130	70	40
24	0	0	0	2	0	360	2.7	130	90	40
Centre point										
25	0	0	0	0	-2	360	2.7	130	80	30
26	0	0	0	0	2	360	2.7	130	80	50
27	0	0	0	0	0	360	2.7	130	80	40
28	0	0	0	0	0	360	2.7	130	80	40
29	0	0	0	0	0	360	2.7	130	80	40
30	0	0	0	0	0	360	2.7	130	80	40
31	0	0	0	0	0	360	2.7	130	80	40
32	0	0	0	0	0	360	2.7	130	80	40

Table 4: Experimental results

I_p(amps)	t_p(sec)	f_p(Hz)	I_b(amps)	S (mm/sec)	TS (MPa)	IS (J)	Hardness (Hv)	Elongation (%)	Bead width (mm)
350	2.4	125	75	45	497	64	391	37	10.22
370	2.4	125	75	35	444	55	368	31	11.13
350	3	125	75	35	441	51	373	30	15.52
370	3	125	75	45	507	45	394	37	13.27
350	2.4	135	75	35	501	46	391	37	16.18
370	2.4	135	75	45	460	52	375	32	11.22
350	3	135	75	45	482	72	369	35	16.04
370	3	135	75	35	478	50	360	34	12.28
350	2.4	125	85	35	462	35	377	32	14.67
370	2.4	125	85	45	480	61	338	34	16.39
350	3	125	85	45	618	48	443	40	10.12
370	3	125	85	35	645	51	376	45	16.64
350	2.4	135	85	45	626	61	380	42	10.92
370	2.4	135	85	35	546	56	382	38	16.91
350	3	135	85	35	660	55	366	47	18.28
370	3	135	85	45	640	45	392	44	11.41
340	2.7	130	80	40	614	55	420	39	14.54
380	2.7	130	80	40	591	52	358	38	10.73
360	2.1	130	80	40	615	65	351	40	12.32
360	3.3	130	80	40	613	56	332	39	15.13
360	2.7	120	80	40	634	52	303	43	10.84
360	2.7	140	80	40	613	50	454	40	17.36
360	2.7	130	70	40	637	52	373	43	10.95
360	2.7	130	90	40	639	56	481	44	10.83
360	2.7	130	80	30	642	50	392	45	19.12
360	2.7	130	80	50	635	62	368	43	11.42
360	2.7	130	80	40	619	48	221	40	10.53
360	2.7	130	80	40	619	48	221	40	10.53
360	2.7	130	80	40	620	48	221	41	11.53
360	2.7	130	80	40	619	48	221	40	10.53
360	2.7	130	80	40	621	48	221	40	10.53
360	2.7	130	80	40	622	49	221	41	11.53

database. TOPSIS , thus, gives a solution that is not only closest to the hypothetically best but also the farthest from the hypothetically worst (Balamurugan *et al*., 2014a, b; Benyounis and Olabi, 2008; Kim and Rhee, 2002; Moon and Na, 1997; Olabi *et al*., 2006; Park *et al*., 2008; Utkarsh *et al*., 2014; Athawale and Chakraborty, 2010; Rahmel *et al*., 1998; Kumar and Ray, 2014; Bhutia and Phipon, 2012). The steps involved in TOPSIS are given below:

Step 1: The given output data's should be normalized with Eq. 1:

$$M_{ab} = Y_{ij}/\left(\sum Y^2_{ij}\right) \text{for } i = 1, \ldots, m; j = 1, \ldots, n \quad (1)$$

Where:

i = Number of alternatives (trials)
j = Number of criteria (output responses)
Y_{ij} = Represents the actual value of the ith value of jth experimental run

Step 2: Weight allocation should be provided for the all criteria outputs. The total sum of weight should be = 1.

Step 3: Design the normalized weighted decision matrix. For example we provide weights for each criteria C_i for i = 1, …, q. Each column of normalized decision matrix by its respective weight values should be multiplied, the obtained element is Eq. 2:

$$D_{ij} = C_j B_{ij} \quad (2)$$

Step 4: Calculate the ideal and negative solution Eq. 3:

$$A^+ = \left\{V_1^+, \ldots, V_n^+\right\} \quad (3)$$

Where:

$$V_j^+ = \left\{\max\left(V_{ij}\right) \text{if } j \in J; \min\left(V_{ij}\right) \text{if } j \in J'\right\}$$

Negative ideal solution Eq. 4:

$$A^- = \left\{V_1^-, \ldots, V_n^-\right\} \quad (4)$$

Where:

$$V^- = \left\{\min\left(V_{ij}\right) \text{if } j \in J; \max\left(V_{ij}\right) \text{if } j \in J'\right\}$$

Step 5: Separate the measured calculated values by TOPSIS method. The obtained value is shown in Eq. 5. The separation from the ideal alternative is:

$$S_i^+ = \left[\sum\left(V_j^+ - V_{ij}\right)^2\right]^{\frac{1}{2}} \qquad i = 1, \ldots, m \quad (5)$$

Similarly, the separation from the negative ideal alternative is Eq. 6:

$$S_i^- = \left[\sum\left(V_j^- - V_{ij}\right)^2\right]^{\frac{1}{2}} \qquad i = 1, \ldots, m \quad (6)$$

Step 6: For a particular alternative, relative closeness as in Eq. 7. Select the option with M_i closest to 1:

$$M_i = U_i^- / \left(U_i^+ + U_i^-\right), \qquad 0 < M_i < 1 \quad (7)$$

RESULTS AND DISCUSSION

TOPSIS implementation

Step 1: First step in TOPSIS method is the normalization of performance of different criterion. This step provides path for comparing different criterion by converting various attributes dimension into non dimensional attribute. By applying (Eq. 1), the calculated normalized matrix is presented in Table 5. Normalize scores or data are as follows:

Table 5: Normalized matrix

Normalized matrix1				
75.19744	13.62249	75.48031	6.154007	1.378331
60.01450	10.06056	66.86146	4.319942	1.634715
59.20624	8.650415	68.69069	4.045731	3.178595
78.25394	6.734753	76.64302	6.154007	2.323772
76.41273	7.037401	75.48031	6.154007	3.454687
64.41781	8.992973	69.42929	4.603143	1.661259
70.72686	17.24097	67.22533	5.506690	3.395161
69.55784	8.314509	63.98603	5.196517	1.989979
64.97918	4.074110	70.17184	4.603143	2.839958
70.14113	12.37532	56.40448	5.196517	3.544946
116.2699	7.662652	96.89194	7.192411	1.351490
126.6513	8.650415	69.80007	9.102895	3.653914
119.2996	12.37532	71.29308	7.929633	1.573610
90.75604	10.42972	72.04551	6.491151	3.773453
132.6106	10.06056	66.13668	9.930022	4.409650
124.6953	6.734753	75.86690	8.702817	1.717999
114.7696	10.06056	87.09210	6.837286	2.789848
106.3323	8.992973	63.27705	6.491151	1.519327
115.1438	14.05152	60.82672	7.192411	2.002964
114.3961	10.42972	54.41973	6.837286	3.020853
122.3683	8.992973	45.32788	8.311730	1.550637
114.3961	8.314509	101.76350	7.192411	3.976959
123.5291	8.992973	68.69069	8.311730	1.582268
124.3060	10.42972	114.22740	8.702817	1.547778
125.4759	8.314509	75.86690	9.102895	4.824224
122.7546	12.78439	66.86146	8.311730	1.721012
116.6465	7.662652	24.11375	7.192411	1.463216
116.6465	7.662652	24.11375	7.192411	1.463216
117.0237	7.662652	24.11375	7.556527	1.754326
116.6465	7.662652	24.11375	7.192411	1.463216
117.4015	7.662652	24.11375	7.192411	1.463216
117.7799	7.985255	24.11375	7.556527	1.754326

$$M_{ab} = Y_{ij}/\left(\sum Y^2_{ij}\right) \text{for} i = 1, \ldots, m; j = 1, \ldots, n$$

Step 2: Allocating weights to the entire criterion which are considered for optimization. The weights considered for this research were; tensile strength = 0.2, impact strength = 0.2, microhardness = 0.2, percentage elongation = 0.2, bead width = 0.2. The sum of weight should be equal to one.

Step 3: Construct the weighted normalized decision matrix. Suppose we have weights for each criteria w_j for j = 1, …, n. On multiplying each column of normalized decision matrix by its respective weight, the element obtained from (Eq. 2) ($D_{ij} = C_jB_{ij}$) Table 6.

Step 4: The next step is determination of ideal and negative ideal solution:

$$A^+ = \left\{V_1^+, \ldots, V_n^+\right\}$$

Where:

$$V_j^+ = \left\{\max\left(V_{ij}\right) \text{if } j \in J; \min\left(V_{ij}\right) \text{if } j \in J'\right\}$$

Negative ideal solution:

$$A^- = \left\{V_1^-, \ldots, V_n^-\right\}$$

Step 5: Separation measure determination is the fifth step in TOPSIS method. The value obtained from (Eq. 5 and 6) is given in Table 7. The separation from the ideal alternative is:

$$S_i^+ = \left[\sum\left(V_j^+ - V_{ij}\right)^2\right]^{\frac{1}{2}} \qquad i = 1, \ldots, m$$

Similarly, the separation from the negative ideal alternative is:

$$S_i^- = \left[\sum\left(V_j^- - V_{ij}\right)^2\right]^{\frac{1}{2}} \qquad i = 1, \ldots, m$$

Step 6: The relative closeness of a particular alternative is calculated from (Eq. 7) and their calculated values are presented in Table 8. Select the option with P_i closest to 1:

$$P_i = S_i^-/\left(S_i^+ + S_i^+\right), \qquad 0 < P_i < 1$$

Optimization of multi performance characteristics: Relative closeness values for each experimental run were calculated using the above mentioned formula (Eq. 7) and

Table 6: Weighted normalized decision matrix

----------Weighted Normalized matrix1----------				
15.03949	2.724498	15.09606	1.230801	0.275666
12.00290	2.012111	13.37229	0.863988	0.326943
11.84125	1.730083	13.73814	0.809146	0.635719
15.65079	1.346951	15.32860	1.230801	0.464754
15.28255	1.407480	15.09606	1.230801	0.690937
12.88356	1.798595	13.88586	0.920629	0.332252
14.14537	3.448193	13.44507	1.101338	0.679032
13.91157	1.662902	12.79721	1.039303	0.397996
12.99584	0.814822	14.03437	0.920629	0.567992
14.02823	2.475063	11.28090	1.039303	0.708989
23.25398	1.532530	19.37839	1.438482	0.270298
25.33026	1.730083	13.96001	1.820579	0.730783
23.85992	2.475063	14.25862	1.585927	0.314722
18.15121	2.085944	14.40910	1.298230	0.754691
26.52211	2.012111	13.22734	1.986004	0.88193
24.93907	1.346951	15.17338	1.740563	0.34360
22.95393	2.012111	17.41842	1.367457	0.55797
21.26646	1.798595	12.65541	1.298230	0.303865
23.02876	2.810304	12.16534	1.438482	0.400593
22.87922	2.085944	10.88395	1.367457	0.604171
24.47365	1.798595	9.065577	1.662346	0.310127
22.87922	1.662902	20.35269	1.438482	0.795392
24.70581	1.798595	13.73814	1.662346	0.316454
24.86119	2.085944	22.84548	1.740563	0.309556
25.09518	1.662902	15.17338	1.820579	0.964845
24.55092	2.556878	13.37229	1.662346	0.344202
23.32929	1.532530	4.822750	1.438482	0.292643
23.32929	1.532530	4.822750	1.438482	0.292643
23.40473	1.532530	4.822750	1.511305	0.350865
23.32929	1.532530	4.822750	1.438482	0.292643
23.48029	1.532530	4.822750	1.438482	0.292643
23.55597	1.597051	4.822750	1.511305	0.350865
26.52221	3.448193	22.84548	1.986004	0.964845
11.84125	0.8414822	4.822750	0.809146	0.270298

Table 7: Separation measure for all the experimental run

S^{+p}	S^{-p}
13.90946	10.93592
17.44354	8.634842
17.4045	8.969691
13.4136	11.19751
13.82719	10.8669
16.44814	9.176623
15.56971	9.318819
16.26033	8.286537
16.39582	9.289136
17.08056	7.035079
5.210889	18.52102
9.132691	16.35591
9.074756	15.38979
11.98405	11.56734
9.725118	17.01051
8.138093	16.72855
6.692935	16.85142
11.62284	12.3042
11.28246	13.54507
12.59831	12.67335
14.04765	13.38942
4.795872	19.08945
9.459861	15.70602
2.259205	22.28952
8.00699	16.88274
9.742243	15.44016
18.42374	11.52765
18.42374	11.52765
18.40676	11.60727
18.42374	11.52765
18.39818	11.67814
18.37514	11.76206

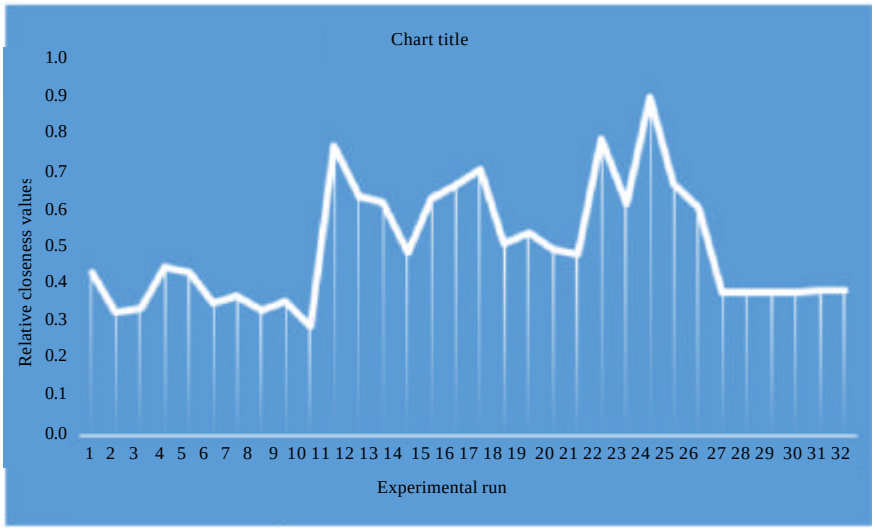

Fig. 3: Graphical representation of experimental runs vs. relative closeness values

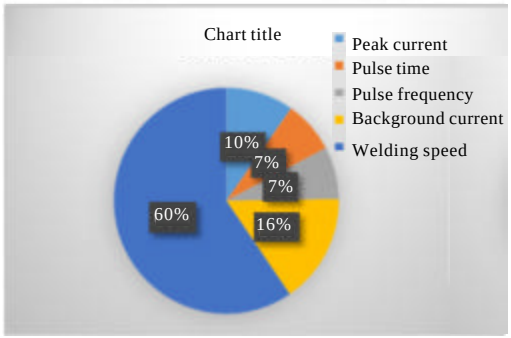

Fig. 4: Percentage of contribution of individual parameters

it was observed that the twenty fourth experimental run had maximum relative closeness value. Relative closeness values for each experimental run are represented in Fig. 3.

ANOVA: In order to analyze the significance and the contribution of each parameter to the closeness coefficient value, ANOVA was carried out and their values are shown in Table 9. This analysis wascarried out for a level of significance of 5%, i.e., for 95% confidence level.

In general when F>4 it means that the change in the process parameter has a substantial influence on the qualitycharacteristic. Therefore, peak current (I_p), pulse time (t_p), pulse frequency (f), back ground current (I_b) and welding Speed (S) have significant influence on the output response. The percentage of contribution of thevarious process parameters is shown in Fig. 4.

Table 8: Relative closeness values

Closeness values	Ranks
0.440159	10
0.331111	22
0.340094	29
0.454978	25
0.440061	27
0.358115	23
0.374422	20
0.337580	26
0.361657	30
0.291723	28
0.780427	2
0.641695	11
0.629065	4
0.491153	24
0.636249	5
0.672731	7
0.715731	16
0.514238	13
0.545567	9
0.501485	21
0.488005	8
0.799213	17
0.6241	6
0.907971	**1**
0.678301	12
0.613133	3
0.384879	16
0.384879	16
0.386728	19
0.384879	15
0.388284	14
0.390284	18

Bold values are significant values

From Table 9 and Fig. 4 it is found that welding speed has more percentage of individual contributing parameter and followed by back ground, peak current, pulse time and pulse frequency.

Table 9: ANOVA of closeness coefficient values

Parameters	Degrees of freedom	Sum of squares	Mean square	F-values	Percentage of contribution
Peak current	4	0.035377	0.00884425	0.30909397	9.76
Pulse time	4	0.027204	0.006801	0.237685286	7.51
Pulse frequency	4	0.027064	0.006766	0.236462085	7.47
Background current	4	0.056934	0.0142335	0.497440599	15.72
Welding speed		0.215588	0.053897	1.883623562	59.53
Error	11	0.429202	0.02861346	3.164305502	
Total	31	0.2381994			

Table 10: Comparative results of conformity test

Experiments	I_p(amps)	t_p(sec)	f_p(Hz)	I_b(amps)	S (mm/sec)	TS (MPa)	IS (J)	Hardness (Hv)	Percentage of elongation	Bead width (mm)
Optimized welding Parameters with predicted values	360	2.7	130	90	40	639	56	481	44	10.83
Experimentally Observed values	360	2.7	130	90	40	645	58	485	45.2	10.73
Percentage of Error	-	-	-	-	-	0.9	3.4	0.82	2.6	0.9

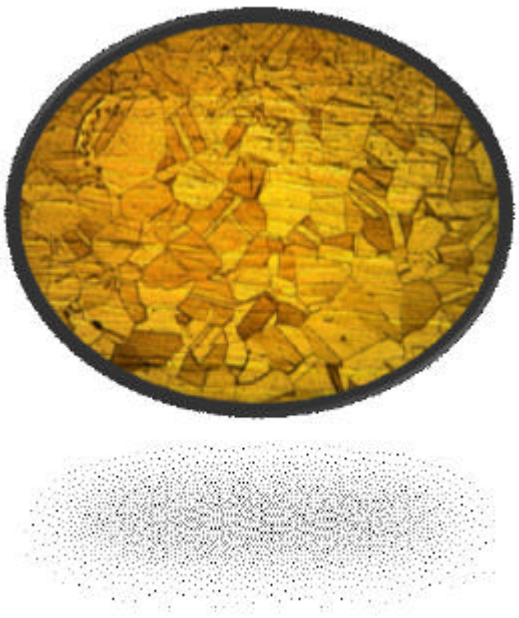

Fig. 5: Base material microstructure

Conformation test: The parameters were optimized through TOPSIS and optimized welding process parameters are peak current-360 amps, pulse time -2.7 sec, frequency-130 Hz, back ground current -90 amps and speed-40 m/min. This optimized parameters are already placed (preliminary trials) on the 24th set of experimental one. Again for the same set of parameters, the trials were conducted and further investigated the mechanical and metallurgical characterization of the optimized set of parameters processed joints. The analysis of the weld bead profiles and tensile, impact and hardness tests were carried out. The macro and tensile test and impact test samples were prepared according to the AWS E 8 substandards and the bead profiles were measured using optical microscopy. The base material microstructure is shown in Fig. 5.

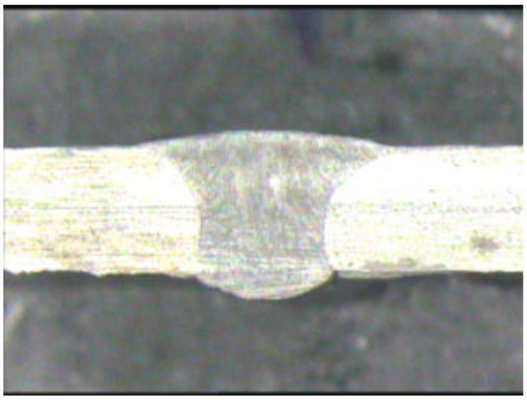

Fig. 6: Bead profile of weld (optimized parameters)

Figure 5 exposes the well defined grain boundaries and also the presence of full austenite phase. The weld bead profile was obtained from optical microscope and bead profiles were measured using image analyser software as shown in Fig. 6.

Figure 6 clearly shows the bead appearance and it is found that full penetration is achieved with narrow heat affected zone. The heat affected zone and weld metal microstructures are presented in Fig. 7a and b.

The grains are very coarser in Fig. 7a and weld metal microstructure (Fig. 7b) grains are finer. Due to high cooling rates, all the weld metals are under equilibrium condition leading to the formation of austenite mode. From the literature Rahmel *et al.* (1998) the apparent presence of two phases was detected and also attributed to the first solidifying grains (dendrites) that were certainly enriched in austenite stabilizing elements while the ferrite stabilizing elements were rejected in the interdendritic liquid. The austenitic stabilizing elements like Ni, N and C first get partioned into primary dendrites (darker phase (Fig. 7b austenite phase). This led to ferrite stabilizing elements like Cr, Mo and Si partitioning into the

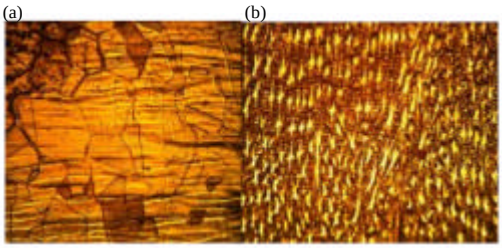

Fig. 7: a) Mmicrostructure of HAZ and b) Weld metal

liquid phase. Along with the elements, partition of impurities was also formed in the liquid and became part of interdendritic (lighter one (Fig. 7a-secondary phase). Figure 7, the grains are finer because of fast cooling rate. The tensile test was performed at room temperature. The transverse tensile strength, yield strength and percentage of elongation of joint were evaluated. Three specimens were tested and the average tensile strength, yield strength and percentage of elongation of each specimen were obtained and the average data was recorded. The welding trials were carried out and the test results were comparedto the predicted values as presented in Table 10. From Table 10 it is observed that the percentage of error is <4% i.e. with in the acceptable range of percentage errors. So, the optimized parameters is prone to give good results i.e., to maximize the tensile strength, percentage of elongation, impact strength, hardness of the welds and minimize the bead width. This may be due to direct effect of back ground current and welding speed. So, the more amount of interdendritic phase that was present in the weld metal would led to increase the strength and toughness of the welds. From Table 10 it is clear that the weld metal tensile strength is much higher with than the predicted set of parameters tensile strength and base metal tensile strength (570 MPa). This is due to the finer grain size present in the weld metal. The tensile tested sample fracture occurred some distance away from the joint in the weld metal. The tensile specimens failed in the base region and it suggests that the weld region is stronger than the base metal region. The SEM fractured surface of the tensile tested microstructure is present in Fig. 8.

Figure 8 shows the fractured surface consists of fine and uniform dimples which indicate that the specimen fails in a ductile manner under the action of tensile loading. The charpy impact toughness values of weld joint were evaluated at room temperature and the results are presented in Table 10. The impact toughness of unwelded base metal is 60 Joules. The optimized set of parameters impact strength is slightly higher than the predicted set of

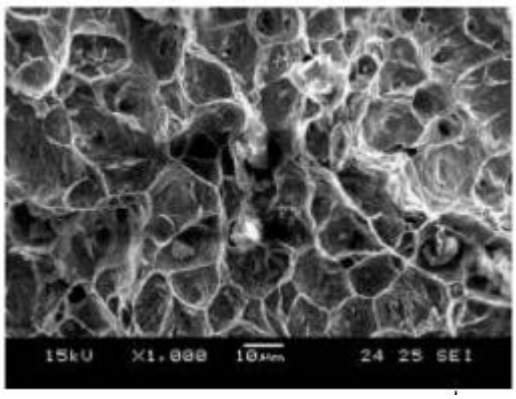

Fig. 8: SEM fractured surface of tensile tested sample

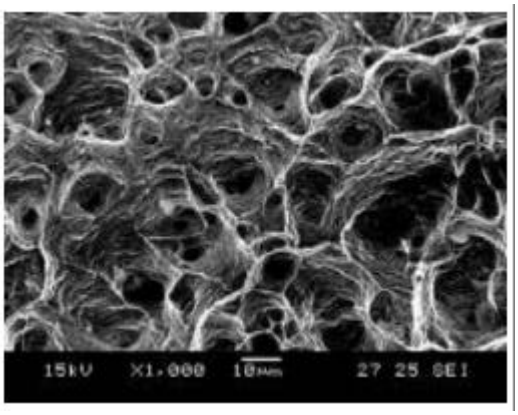

Fig. 9: SEM fractured surface of impact tested sample

parameters impact strength. The fractured surface of impact specimens are analyzed using SEM. The fractured surface of the impact tested fractrograph is shown in Fig. 9.

From Fig. 9 it is observed that elongated and fine dimples are clearly seen. Fine dimples are a characteristic feature of a ductile mode of fracture. The dimple size exhibits a directly proportional relationship with strength and ductility that is if the dimple size is finer, then the strength and ductility of the respective joint is higher and vice versa. The impact specimen fracture surfaces of the P-GMAW welded joints show mixed mode fractures that is ductile and cleavage fractures. The hardness across the weld cross section was measured using a Vickers Micro Hardness testing machine and the results are shown in Table 10. The hardness of the weld region is greater than that of the predicted set of parameters hardness and base metal. It is due to low heat input with rapid cooling and it can promote the finer grain size in the weld metal. Due to fine grain size the weld metal hardness values are much higher than the base metal. The hardness

values increase moving from the base material across the weld joint towards its opposite side. This may be the result of the effect of rapid solidification. Rapid solidification increases under cooling and nucleation probability leads to very fine microstructure. The experimentally obtained bead width is lesser than the predicted obtained bead width. This is due to more amount heat transferred in the perpendicular direction and less of heat transferred in the longitudinal direction.

CONCLUSION

Based on the P-GMAW parameters (AISI 904 L SASS) considered in this study, the following points are deduced:

The optimization of P-GMAW by calculating the TOPSIS and using the recommendation for determining welding parameters was successful.

Based on ANOVA results, TOPSIS method isan accurate technique to optimize the P-GMAW process in order to obtain good tensile strength, percentage of elongation, impact strength and weld metal hardness and also less bead width.

From TOPSIS method, percentage contribution of individual parameters were determined and found that welding speed has more percentage of individual contributing parameter followed by back ground, peak current, pulse time and pulse frequency. The confirmation test is carried out and the predicted results are very closer to the experimental results (error <4%).

The weld metal consists of primary dendrite and secondary interdendritic phases. The grains are very finer in the weld metal than the HAZ. The percentage of secondary interdendritic phases are higher in the weld metal.

Due to finer grain size (predicted set of parameters) the toughness and hardness of the welds are higher than the experimentally obtained values.

The optimized parameters are prone to give good results i.e., to maximize the tensile strength, percentage of elongation, impact strength, hardness of the welds and minimize the bead width of the weld bead.

ACKNOWLEDGEMENT

The researchers would also like to thank the Dept. of Manufacturing Engineering, Annamalai University, Annamalai Nagar for the continous support. The researchers would like to thank the reviewers and the editor of the journal for their helpful comments which have greatly improved this study.

REFERENCES

Athawale, V.M. and S. Chakraborty, 2010. A TOPSIS method-based approach to machine tool selection. Proceedings of the International Conference on Industrial Engineering and Operations Management, January 9-10, 2010, IEOM, Dhaka, Bangladesh, pp: 1-6.

Balamurugan, K., J.V. Elies, P. Sathiya and A.N. Sait, 2014a. Optimization of friction welding parameters of AISI 904L super austenitic stainless steel by evolutionary computational techniques. Mater. Test., 56: 245-250.

Balamurugan, K., M.K. Mishra, P. Sathiya and A.N. Sait, 2014b. Weldability studies and parameter optimization of AISI 904L super austenitic stainless steel using friction welding. Mater. Res., 17: 908-919.

Benyounis, K.Y. and A.G. Olabi, 2008. Optimization of different welding processes using statistical and numerical approaches- A reference guide. Adv. Eng. Software, 39: 483-496.

Bhutia, P.W. and R. Phipon, 2012. Application of AHP and TOPSIS method for supplier selection problem. IOSR. J. Eng., 2: 43-50.

Chellappan, M., K. Lingadurai and P. Sathiya, 2017. Characterization and optimization of TIG welded supermartensitic stainless steel using TOPSIS. Mater. Today Proc., 4: 1662-1669.

Kim, D. and S. Rhee, 2002. Design of a robust fuzzy controller for the arc stability of CO2 welding process using the Taguchi method. IEEE. Trans. Syst. Man Cybern., 32: 157-162.

Kumar, R. and A. Ray, 2014. Selection of material for optimal design using multi-criteria decision making. Proc. Mater. Sci., 6: 590-596.

Moon, H.S. and S.J. Na, 1997. Optimum design based on mathematical model and neural network to predict weld parameters for fillet joints. J. Manuf. Syst., 16: 13-23.

Olabi, A.G., G. Casalino, K.Y. Benyounis and M.S.J. Hashmi, 2006. An ANN and Taguchi algorithms integrated approach to the optimization of CO2 laser welding. Adv. Eng. Software, 37: 643-648.

Park, H.J., D.C. Kim, M.J. Kang and S. Rhee, 2008. Optimisation of the wire feed rate during pulse MIG welding of Al sheets. J. Achiev. Mater. Manuf. Eng., 27: 83-86.

Rahmel, A., H.J. Grabke and W. Steinkusch, 1998. Carburization-introductory survey. Mater. Corros., 49: 221-225.

Sathiya, P., K. Panneerselvam and R. Soundararajan, 2012. Optimal design for laser beam butt welding process parameter using artificial neural networks and genetic algorithm for super austenitic stainless steel. Opt. Las. Technol., 44: 1905-1914.

Sathiya, P., M.A. Jaleel, D. Katherasan and B. Shanmugarajan, 2011. Optimization of laser butt welding parameters with multiple performance characteristics. Opt. Laser Technol., 43: 660-673.

Sathiya, P., P.M. Ajith and R. Soundararajan, 2013. Genetic algorithm based optimization of the process parameters for gas metal arc welding of AISI 904 L stainless steel. J. Mech. Sci. Technol., 27: 2457-2465.

Utkarsh, S., P. Neel, M.T. Mahajan, P. Jignesh and R.B. Prajapati, 2014. Experimental investigation of MIG welding for ST-37 using design of experiment. Intl. J. Sci. Res. Publ., 4: 1-4.